



Revisiting the effect of extreme flooding on the chemistry of a large floodplain river: the example of Argentina's middle Paraná

P. J. Depetris¹

Received: 7 March 2020 / Accepted: 17 November 2020 / Published online: 11 January 2021
© Springer-Verlag GmbH Germany, part of Springer Nature 2021

Abstract

The multinational Paraná River (drainage basin $\sim 2.6 \times 10^6$ km²; current discharge ~ 540 km³ y⁻¹) has in its middle and lower stretches a long (~ 1200 km) and wide ($\sim 30 - 50$ km) flood valley mantled with riparian vegetation and fully carved with lentic and lotic water bodies. Most of the wetland (~ 50000 Km²) holds myriad water bodies which, following the seasonal variation of the prevailing discharge regime, exchange water, dissolved chemical species, sediment, and biological materials with the Paraná's main stem. Exceptional hydrological events (e.g., strong El Niño-triggered floods) sporadically inundate almost totally the flood valley's expanse. The examination of chemical data collected in the main channel during the 1982–1983 event showed: (a) TDS was diluted to almost $\frac{1}{4}$ of the original concentration during the high flood; (b) water pH decreased to ~ 6.5 , and CO₂ partial pressure increased up to ~ 16000 ppmv during the overbank stage and afterwards; (c) throughout the event water remained within the *medium dilute/dilute* water types ($375 > \text{TZ}^+ > 1500$ $\mu\text{eq L}^{-1}$); and (d) dissolved inorganic carbon (DIC)—along with other variables—reached the highest concentrations in the descending limb, when the floodplain was drained. Dissolved organic carbon (DOC) showed an uneven variability pattern, seemingly unrelated to DIC, but definitely influenced by the significant lentic–lotic exchange. A 10-year long (1965–1975), uninterrupted series of alkalinity measurements allowed probing into the mechanisms that contributed to determine the observed alkalinity variability. Such variation appeared controlled by several biogeochemical processes occurring in the wetland (e.g., photosynthesis/respiration), sporadically impacted by changing hydrological stages.

Keywords Floodplain · Wetland · Flood regime · Alkalinity · ENSO effect · Biogeochemistry · Hysteresis

Introduction

Rivers construct floodplains through a combination of erosion and deposition at lower gradient stretches of river valleys. A floodplain is a relatively low relief sedimentary plain, although it has a general downstream slope coherent with

the overall river gradient. In large rivers, floodplains usually have a “topographic amplitude between ridges and the beds of floodplain water bodies of ~ 0.1 – 0.5 times the bank full depth of the river, constructed by various sedimentation processes and inundated to some extent by most annual floods in the current hydro climatic regime of the river's drainage basin” (Dunne and Aalto 2013). Floodplains are filled with alluvium (i.e., loose sediments transported by streams), which is easily eroded and redeposited by the river. It follows that the location in a floodplain of a river main channel is not a stable feature and changes with a measurable rate (e.g., Paira and Drago 2007).

Flooding, besides being a normal characteristic of river behavior, occurs when the water depth in a river exceeds the depth of the waterway and spreads beyond the river main channel onto the surrounding land (e.g., Benke et al. 2000; Steiger et al. 2005). When a river fills completely its main stem, it is said to be at bank full stage; when it surpasses bank full stage it is said to be an overbank flood.

This article is a part of the Topical Collection in Environmental Earth Sciences on “Advances in Environmental Geochemistry” guest edited by Dr. Eleanor Carol, Dr. Lucia Santucci and Dr. Lia Botto.

Supplementary Information The online version contains supplementary material available at <https://doi.org/10.1007/s12665-020-09309-4>.

✉ P. J. Depetris
pedro.depetris@gmail.com

¹ Academia Nacional de Ciencias, Avenida Vélez Sarsfield 229 – 249, X5000WAA Córdoba, República Argentina

Abundant literature shows that flooding dynamics are considered to be the chief variable forcing the structure and functioning of floodplain systems (Dunne and Aalto 2013, and references therein). Overbank events force longitudinal, vertical, and lateral exchanges of material and energy, finally affecting—among several other impacts—patterns of sediment deposition and erosion (e.g., Potter et al. 2005), and biogeochemical cycling through space and time (e.g., Richards et al. 2003; Tank et al. 2010). Moreover, the time in which a floodplain remains inundated depends on the size of the river, its slope, and the prevailing climatic characteristics. Excess water is eventually disposed of by downstream drainage, water infiltration, and evapotranspiration.

To attain such goal, a partly unpublished data set produced within the framework of the SCOPE-UNEP International Carbon Project (e.g., Degens et al. 1991) was herein employed, seeking to analyze the interrelationship between high discharges (i.e., outstanding overbank events) and the resulting impact on solute concentrations (particularly addressing alkalinity dynamics), in the middle Paraná River, Argentina, which is characterized by a vast floodplain. The data suite includes the occurrence of an exceptional ENSO-triggered overbank flood, involving samples collected between 1981 and 1984, near the Argentine city of Paraná, ~600 km upstream the mouth. Also included and within the same project, there is another data array, collected in 1985, in an expanded downriver survey.

The data series collected within the carbon project was supplemented with another set, here used to explore the fluvial processes affecting alkalinity dynamics. Based on continuous, uninterrupted daily analyses gathered during a decade, the hydro chemical data were collected by Argentina's *Obras Sanitarias de la Nación* in approximately the same sampling spot used in the previously mentioned series (i.e., ~600 km upstream the mouth). The series comprises hydrological and chemical data, recorded between 1965 and 1975, and—taking advantage of its extended and continuous characteristics—it is used to probe further into the association existing between alkalinity, and the floods (i.e., some of exceptional magnitude) that periodically inundate the ample flood valley of the Paraná River's middle range.

Main features of the Paraná River

The Paraná River and its tributaries account for the largest proportion (~81%) of the Río de la Plata drainage basin (~3.17 10⁶ km²), pertaining the remainder area to the Uruguay River drainage basin (Fig. 1). In terms of basin area (~2.58 10⁶ km²), the Paraná River occupies the fifth place among the global rivers that discharge more than 400 km³ of water annually (Milliman and Farnsworth 2011). It is 4500 km-long and drains a continental-sized



Fig. 1 Map of the Río de la Plata drainage basin, comprised by the Paraná and Uruguay rivers. The ~800-Km long Paraná's middle reach is defined between the cities of Corrientes and Rosario (red arrows). All the samples referred to in this article were collected near the city of Paraná (i.e., blue arrow, ~600 km upstream the mouth, 32° 39' 59" S, 60° 47' 36" W). The stage meter at La Paz is located 337 km north of Rosario (Wikipedia Commons)

drainage basin formed by several contrasting regions in four different countries (i.e., Brazil, Paraguay, Bolivia, and Argentina), with an assortment of mountain chains, rainforests, deserts, and savannas (Fig. 1), thus configuring a dissimilar scenario: from Andean sources close to South America's Pacific active margin, in the Bermejo and Pilcomayo upper catchments (~65°W), to the tropical headwaters placed at the *Serra dos Preneos* (~45°W), close to the Atlantic passive margin. The *Gran Pantanal* (i.e., 0.2 × 10⁶ Km², one of the largest wetlands in the world at ~15°–17°S, and ~55°–60°W) is an additional headwater that exerts a discernible modulating effect on the Paraguay River, which joins the Paraná near the Argentine city of Corrientes, where its middle reach begins.

Maximum precipitation (2400 mm y⁻¹) occurs along the eastern edge of the basin and over the Iguazu River drainage basin. Rainfall decreases (400–800 mm y⁻¹) towards the western edge, along the 60–65°W strip. In general, runoff mimics rainfall distribution, with high values along the drainage basin's NE corner (700–800 mm y⁻¹), and in the Bermejo and Pilcomayo upper catchments (~500 mm y⁻¹). In Argentine territory, the Paraná's upper and middle course has a mean runoff of ~300 mm y⁻¹. Potential evapotranspiration at the origin of Paraná's middle course is ~1000 mm y⁻¹ and gradually decreases to 850 mm y⁻¹, at the mouth.

Most of the Paraná River drainage network seems to have originated in the Late Cretaceous, in synchrony with the opening of the Atlantic Ocean. Its mouth, however, switched to the present Río de la Plata estuary, about 2.4 My. Its structural setting is a classic intra-cratonic layout for much of its course; its main geological features are defined by Upper Paleozoic and Mesozoic sediments and extensive volcanic flood-basalts constrained by Precambrian crystalline rocks (Potter and Hamblin 2006).

The Paraná basin's hydrographic net is a complex system that transports water down to the middle latitudes of the South Atlantic Ocean, collecting and modifying inorganic and organic materials from mountainous as well as from low-relief tropical environments. Iriondo et al. (2007) have dealt extensively with the Paraná's features, in general, and particularly with those of its middle stretch.

Data and methods

Argentina's *Sistema Nacional de Información Hídrica* allows to download permanently updated Paraná River discharge data from different discharge (or stage height)-measuring stations placed along the Paraná main stem and tributaries (<https://snih.hidricosargentina.gov.ar/Inicio.aspx>). As indicated in the text, data from four gauging stations (i.e., Corrientes, La Paz, Paraná, and Rosario) placed along the Paraná's main channel have been used throughout this paper.

Parametric statistics, such as regression and correlation analysis, require that the variables under study adjust to a normal distribution. Discharge and solute concentrations often show a skewed statistical distribution, which can be normalized by converting to logarithms. This procedure has been followed wherever necessary.

Discharge data were deseasonalized by subtracting the mean historical discharge of a specific month from the measured discharge for the same month in the data series: $Q_{iD} = Q_i - Q_{mi}$, where Q_{iD} is the deseasonalized discharge of the i th month; Q_i is the measured mean monthly discharge for the i th month, and Q_{mi} is average historical discharge for the i th month.

The downriver flood wave velocity—between the stage meters placed at La Paz (757 km upstream the mouth) and Rosario (420 km upstream the mouth) during the 1982–1983 ENSO triggered outstanding flood—was determined by employing the cross-correlation statistical technique (e.g., Davis 1986). The method is appropriately used to compare two time-dependent series, thus revealing the strength of such relationship, and the lag or offset in time between them at their position of maximum equivalence.

Water surface slopes (WSS) were determined using the water heights recorded in the stage meters placed at La Paz (757 km upstream Paraná's mouth) and at the city of Rosario (420 km upstream Paraná's mouth). Both parameters are also

reported by the *Sistema Nacional de Información Hídrica* of Argentina. The employed simple equation was, $S_{WSS} = (H_{LP} - H_R)/D_{LP-R}$, where S_{WSS} is the WSS, H_{LP} and H_R are La Paz and Rosario stage meter readings, respectively, and D_{LP-R} is the distance between La Paz and Rosario (337 km). The relative gauging station heights were transformed to sea-level values by applying the corresponding numerical corrections (Soldano 1947).

As stated above, three different data suites have been used to tackle this paper's subject matter. They were the only available data series for the Paraná River, which contained physicochemical information associated with river discharge measurements. The main data set was gathered between 1981 and 1984 in the middle Paraná, sampled 600 km upstream the mouth during the progress of the SCOPE-UNEP International Carbon Project. This data set was accompanied with another array obtained in a downriver exploration (Depetris and Kempe 1993), from the Iguazu falls (i.e., 1927 km upstream the mouth), down to the dock of the city of Paraná (i.e., 600 km upstream the mouth). This project, which had its main seat at *Universität Hamburg* (Hamburg, Germany), was originally initiated to gather detailed information on the dynamics of inorganic and organic carbon species in world rivers (e.g., Degens et al. 1991, and references therein). The methodologies for various methods used in the field, anions, cations, and assorted carbon species have been described by Michaelis and Ittekkot (1982). Data on the main inorganic constituents are reported here for the first time, whereas the riverine dynamics of various carbon species has been dealt with elsewhere (Depetris and Kempe 1993).

The *Aqion*¹ hydrochemistry software (<https://www.aqion.de/site/98>) was employed to check for charge balance errors (CBE) and to calculate several variables (e.g., TDS, Eh, ionic strength, etc.). Most CBE in both data sets assembled within the framework of the SCOPE-UNEP International Carbon Project fluctuated between –4.7% (deficiency of cations) and 4.9% (deficiency of anions).

The added data series was selected based on the need of using a long and uninterrupted data series to probe into the mechanisms linking alkalinity with the level reached by water in the floodplain (i.e., discharge variability). A 10-year long time series (1965–1975) of *daily chemical analyses* performed in the Paraná River (Lenardón 1979), at the city of Paraná, sampled about 600 km upstream from the mouth, was used to probe into the hydrology–alkalinity relationship. The chemical analyses were performed in the laboratories of *Obras Sanitarias de la Nación*, Argentina's federal agency

¹ This software used to validate aqueous solutions operates with the well-known USGS's PhreeqC as an internal numerical solver.



Fig. 2 Image of a portion of the middle Paraná River flood valley. Notice the profusion of anastomosed lotic and lentic water bodies that dissect the riparian environment; clear ponds have not been flooded in the immediate past (i.e., particulate matter has settled down). The distance from top to bottom of the figure is ~30 km (Wikipedia Commons)

which, at that time, was in charge of the daily quality control of river water, subsequently processed to attain potable quality, and distributed for human consumption through municipal networks.² Monthly concentration (geometric) means were calculated from daily measurements. This extended series included several chemical parameters, which were determined simultaneously (i.e., pH, TDS, color, turbidity, water hardness, sulfate, alkalinity, chloride, etc.), permanently subjected to strict quality controls. However, only alkalinity and chloride concentrations were employed in this work. Alkalinity was determined by standard 0.1 N H₂SO₄ electrometric titration; precision was checked every ten samples, and was within 2.1% ($p < 0.001$). The well-known Mohr method (i.e., titration with a AgNO₃ solution) was used to measure Cl⁻ concentrations; precision was checked every 20 samples, and was within 1.9% ($p < 0.001$). Lenardón (1979) supplied more detailed analytical information.

Hydrological outline of the Paraná River

The Paraná's middle reach originates when the river—with headwaters in tropical Brazil—meets the Paraguay River, near the Argentine city of Corrientes (i.e., 1208 km upstream the mouth), and extends downstream for ~800 km (i.e., until the city of Rosario), with a floodplain width that fluctuates between ~20 and ~50 km (Fig. 2). Although it accounts for about ~1.5% of the total drainage basin's area, the extensive wetland is important in terms of biodiversity and as a significant factor affecting the riverine biogeochemistry.

Countless lentic and lotic water bodies of assorted shape, size, and age fill the middle Paraná floodplain (Fig. 2).

² The sanitary services delivered by Argentina's *Obras Sanitarias de la Nación* were privatized in 1992.

Modern and evolved meanders, and anastomosed plains are the main geomorphological units (Paira and Drago 2007). These features are embedded in a heterogeneous mosaic of water bodies, with landscapes determined by the variable dynamics of the fluvial processes, and the short- and long-term evolution of the river floodplain (Fig. 2). The Paraná's floodplain is inundated and partially drained periodically following the river's seasonal discharge variability. A flood may barely enter the floodplain or—when reaching a very high stage—it may inundate entirely the distance across the riparian environment. Excess water on the floodplain drains back to the channel as the river discharge recedes. On wide floodplains—such as the Paraná's—bordered by natural levees, the water may drain back slowly, causing local inundation or pounding which may last for months.

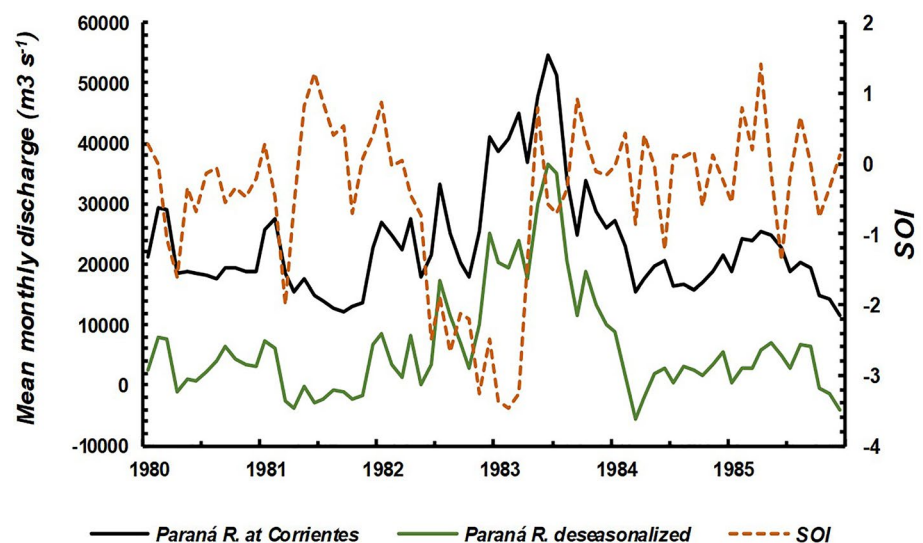
The Paraná River currently delivers to the SW Atlantic a mean discharge of ~17000 m³ s⁻¹ (i.e., ~540 Km³ annually), and shows a statistically significant increasing discharge trend since the 1970s, as well as an active remote connection with El Niño-Southern Oscillation (ENSO) events in the Pacific Ocean (e.g., Depetris et al. 1996; Pasquini and Depetris 2007, 2010). The teleconnection linking the Southern Oscillation (SO) and Paraná River discharges was originally recognized by Sir Gilbert Walker's research group, back in the 1920s, when they were pursuing the prediction of India's monsoons (e.g., Depetris et al. 1996, and references therein). The El Niño occurrence in the Pacific Ocean frequently triggers—among several other global climatic impacts—exceptionally abundant rainfalls in the Brazilian headwaters of the upper Paraná and Paraguay rivers. Since El Niño episodes are usually in phase with the Paraná's seasonal high-water period (i.e., during December–March, the austral summer), its occurrences frequently result in overbank floods—sometimes of exceptional magnitude. La Niña events, on the other hand, often result in below-the-mean discharges, usually during the southern summer.

An aspect worth emphasizing is that, although the upper Paraná River provides an average of ~70% of the water reaching the river's middle reach (Pasquini and Depetris 2007), the Paraguay River increased its relative discharge contribution to the middle section of the Paraná River, during the 1982–1983 high flood (Pasquini and Depetris 2010). However, most of the total suspended sediment (TSS) load being transported to Corrientes is delivered by the Paraguay River and, particularly, by one of its Andean tributaries, the Bermejo River (e.g., Campodonico et al. 2016, and references therein).

Figure 3 shows the Paraná River monthly mean discharge for the period 1980–1985, along with the corresponding deseasonalized discharge series and the Southern Oscillation Index (SOI)³ (e.g., Stone et al. 1996, Sarachik and Cane

³ The Southern Oscillation Index (SOI) is a measure of the strength of the Walker Circulation, and one of the key atmospheric indices for

Fig. 3 Mean monthly and deseasonalized discharge of the Paraná River at Corrientes (1208 km upstream the mouth), for the period 1980–1985. The Southern Oscillation Index (SOI) (i.e., one of the key atmospheric indices for gauging the strength of El Niño and La Niña events) is also included in the graph to show the connection between the 1982 and 1983 ENSO event in the equatorial Pacific and the occurrence of one of the highest floods on record



2010). The figure shows the markedly negative SOI value, which preceded the exceptionally high ENSO-caused flood of 1982–1983 in the Paraná River, the highest on record (e.g., Hansen 1990). The flood began in 1982 and lasted for almost 2 years, reaching a peak discharge which nearly touched $60000 \text{ m}^3 \text{ s}^{-1}$ at the Corrientes gauging meter, almost four times the Paraná River average annual discharge. The inundation flooded the areas that the USA's FEMA (Federal Emergency Management Agency) designates as between the limits of the 100-year and 500-year floodplain (i.e., with a 0.2% annual chance of flooding, affecting areas beyond the protection of levees from 100-year flood).

The deseasonalized data series allows to assess further the flood impact. During the considered period (1980–1985), the deseasonalized discharge shows that, at the flood's peak, it exceeded by $\sim 37000 \text{ m}^3 \text{ s}^{-1}$ the historical average discharge for the same period (Fig. 3). This discharge meant a gauge stage height of $\sim 9 \text{ m}$, i.e., several meters above the mean hydrograph value at the Corrientes stage meter. It is worth considering that the mean annual (historical) discharge at Corrientes is reached when the stage meter height is $\sim 3.2 \text{ m}$ ($\sim 17000 \text{ m}^3 \text{ s}^{-1}$). River water enters or is flushed out of the lentic/lotic environments - overly abundant in the flood plain - when stage readings fluctuates in the $\sim 2.9\text{--}3.3 \text{ m}$ range. A high flood (e.g., $\sim 45000 \text{ m}^3 \text{ s}^{-1}$) reaches a stage reading of $\sim 7 \text{ m}$ at Corrientes, covering extensive areas of the riparian zone with more than a $\sim 3 \text{ m}$ -deep water mass. A conservative estimate proposes that during the 1982–1983 flooding period (~ 18 months), the valley stored between 200

and 400 km^3 of water, which probably signified a contribution of $\sim 10\text{--}20\%$ to the topmost discharges.

The velocity of propagation of the flood-wave in the middle section of the Paraná River - when the flood reaches a middle stage in the rising limb - is $\sim 60 \text{ km d}^{-1}$, and it slows down to $\sim 45 \text{ km d}^{-1}$, or less, during the high or very high stage (Soldano 1947). By means of the cross-correlation method, it was possible to establish that, during the 1982–1983 ENSO high flood, it took 9 days to the flood wave to cover the distance (337 km) that separates the stage meters of La Paz (i.e., 757 km upstream the mouth) and Rosario (i.e., 420 km upstream the mouth), progressing downriver at a mean velocity of $\sim 49 \text{ km d}^{-1}$ (i.e., $\sim 0.6 \text{ m s}^{-1}$). The flood wave, which is slower than the mean water velocity in the main channel, clearly affects the water surface slope (WSS).

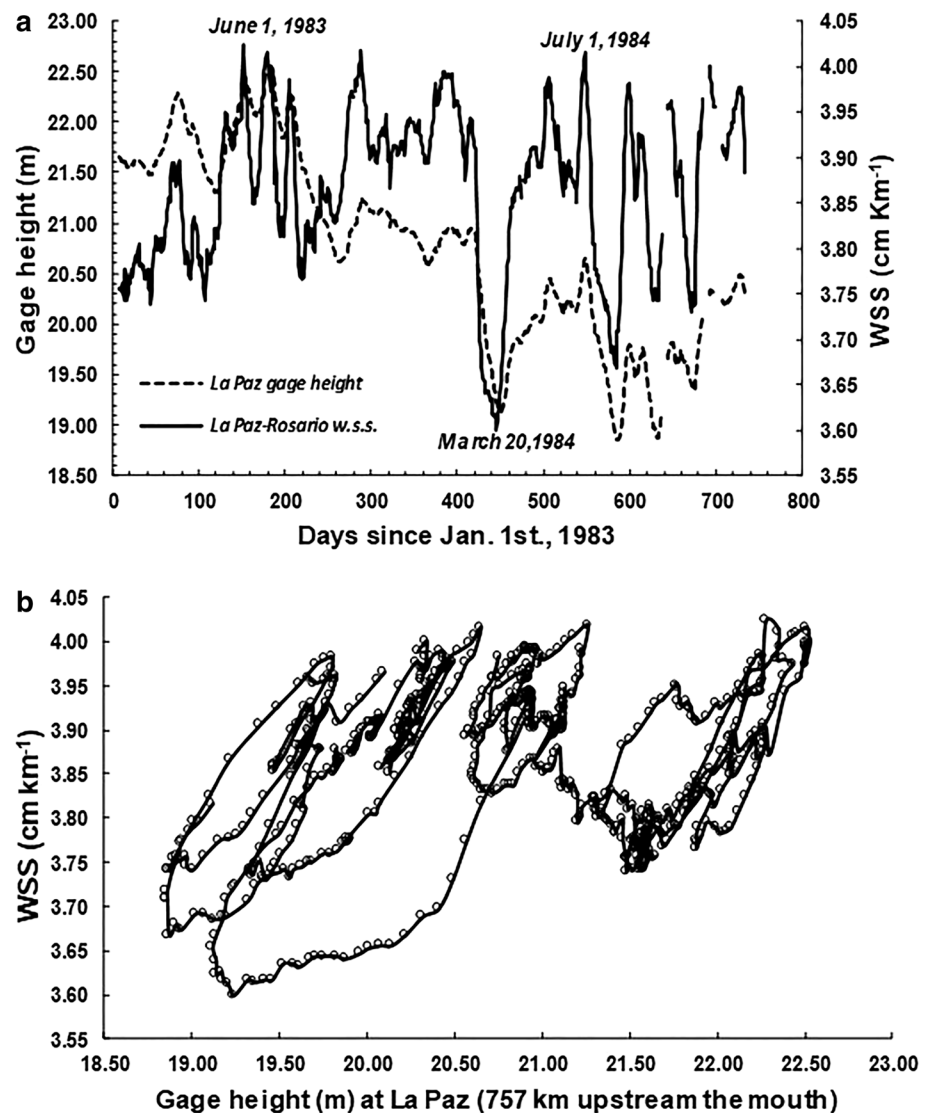
The gauge oscillations inherent to the WSS determine the influx or outflow of flood water in the flood plain (Fig. 4). Figure 4a shows that the relationship between discharge (i.e., stage meter height at La Paz) and WSS is a complex one, because WSS may increase with increasing stage readings (e.g., as in the peaks of June 1983) but, also, with decreasing ones, as of July 1, 1984 (Fig. 4a). The latter instance implies that, with decreasing stage heights, the floodplain was being drained due to increased WSS. Conversely, the plunging discharge as of March 20, 1984 (Fig. 4a) appears to determine a significant decrease in WSS, which probably marks a slowed-down draining of the floodplain. At any rate, the draining of the wetland occurs when water level at the main channel descends significantly and WSS maintains a relatively high value (e.g., $\text{WSS} > 3.8 \text{ cm km}^{-1}$).

It seems clear that the residence time of flood water in the floodplain was of the order of days/weeks during the inundation of 1982–1983, but it can extend months—or even years—during extended periods of low waters, when lentic environments become practically isolated from the main

Footnote 3 (continued)

assessing the strength of El Niño (i.e., negative index) and La Niña events (i.e., positive index).

Fig. 4 **a** The 1982–1983 Paraná River high flood. **a** Variability of the gage height at La Paz (i.e., 757 km upstream the mouth) and the corresponding water surface slope (WSS) between La Paz (i.e., 757 km upstream the mouth), from Jan. 1st 1983 until Jan. 4th 1985), and Rosario (i.e., 420 km upstream the mouth). The channel slope between both localities is $\sim 3.7 \text{ cm km}^{-1}$. Notice high WSS coherent with low gage height. The draining of the floodplain is promoted when discharge is on the descending limb and $\text{WSS} > 3.8 \text{ cm km}^{-1}$. **b** Hysteresis between gage height (at La Paz) and the WSS between La Paz and Rosario. High and low discharges define a marked amplitude variability for the corresponding WSS loops



lotic ones. On the other hand, the scatter graph of Fig. 4b displays the complex connection—known as *hysteresis*—between stage meter height (i.e., discharge) and WSS, at the stage meter of La Paz.

River discharge, soil moisture tension, solute and suspended sediment concentrations experience the occurrence of hysteresis (e.g., Walling and Webb 1988, Baca 2008). However, some aspects of such looped rating curves still remain unclear (e.g., Muste and Lee 2013). Hysteresis in river discharge is most pronounced in flat sloped streams and occurs during unsteady flow when WSS changes due to either rapidly rising or falling water levels in a river control reach. The loops suggest the occurrence of *rate-dependent hysteresis* (i.e., a dependence of the state of the system on its history),⁴ which shows smaller loops as the discharge

increases (i.e., narrower WSS variability), and wider loops in the opposite situation, thus reflecting differences in the dynamics of the water exchange between the riparian zone and the lotic systems (Fig. 4).

The described dynamic water exchange between the main river stem and the extensive floodplain not only leads to significant ecological impacts but also affects the relationship between water volume and solutes or suspended particle concentrations. When large water masses, that have been stored in the floodplain for weeks or months—and, hence, subjected to numerous processes that alter their physico-chemical characteristics—re-enter the main channel while undergoing a receding stage, the chemical and physical characteristics of flowing water in the main stem may change, sometimes markedly.

⁴ In mathematical terms, the response to an external effect is a doubled-valued function. One applies when the effect is increasing, while the other operates when the influence is decreasing.

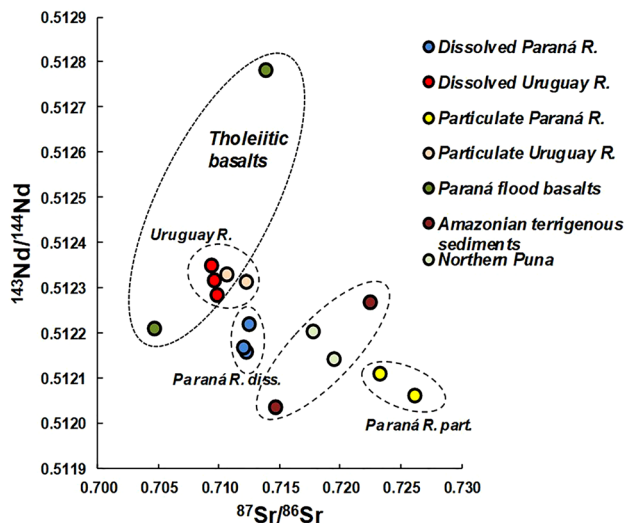


Fig. 5 Scatter graph for $^{87}\text{Sr}/^{86}\text{Sr}$ and $^{143}\text{Nd}/^{144}\text{Nd}$ signifying different sources for the Paraná River solid and dissolved phases. Additional data included for comparison

Results and discussion

The geochemical (e.g., Sanci and Panarello 2018; Campononico et al. 2015, 2016; Depetris and Pasquini 2007; Pasquini and Depetris 2012; De Cabo and Seoane 2005; Depetris 1976), and biogeochemical characteristics (e.g., Ceballos et al. 2013; Depetris 2005; Villar et al. 1998; Depetris and Kempe 1993; Depetris and Paolini 1991) of the Paraná River have been studied for several decades. The vast and intricate wetland that comprises its middle reach has received special attention not only due to the complexity of its ecosystem, and to partly clear biogeochemical features, but also because there is a need to improve knowledge on its functioning, of utmost importance when human intervention must be dealt with.

The geochemical signature of dissolved and particulate phases

Dissimilar geology, climate, topography, and biota characterizes each of Paraná's three main headwaters (i.e., Andean Bermejo and Pilcomayo rivers; Paraguay's *Gran Pantanal*, and upper Paraná's tropical mountainous ranges), and such attributes results in different geochemical features in the total suspended solids (TSS) as well as in the dissolved phases. The middle Paraná sediment load bears a signature of one source supplying "old or recycled materials affected by intracrustal differentiation", and a secondary source of "young material derived from undifferentiated volcanic rocks" (Compononico et al. 2016). This is also succinctly shown by radiogenic isotopic data. Figure 5 shows differing isotopic signatures in the Paraná River for the dissolved and particulate species, whereas

the Uruguay River samples (i.e., included for comparison), with a relatively uniform lithology (i.e., dominant tholeiitic flood basalts), do not (Henry et al. 1996). Paraná River TSS is significantly more radiogenic (e.g., $^{87}\text{Sr}/^{86}\text{Sr}$, 0.723–0.726) than its dissolved counterpart, and has low $^{143}\text{Nd}/^{144}\text{Nd}$ ratios (e.g., 0.5120–0.5121, and negative ϵ_{Nd} (0)), typical of an enriched crustal source. Conversely, the dissolved fraction is somewhat less radiogenic (e.g., $^{87}\text{Sr}/^{86}\text{Sr}$, 0.7120–0.7124), maintaining a negative ϵ_{Nd} (0) and lower $^{143}\text{Nd}/^{144}\text{Nd}$ ratios (e.g., 0.5120–0.5122) (Henry et al. 1996). These isotopic differences are probably related to the diverse sources supplying the largest proportion of the sediment load (i.e., the Bermejo River) and the major water source (i.e., the upper Paraná drainage basin). Data from the southern Puna (Gili et al. 2017) and from Amazonian sediments (Rollinson 1993) plot halfway between both clusters. Contrastingly, the Uruguay River data are compatible with Paraná flood basalts (Faure 1986), and does not show significant differences in its isotopic signatures, regardless of its particulate or dissolved nature (Fig. 5).

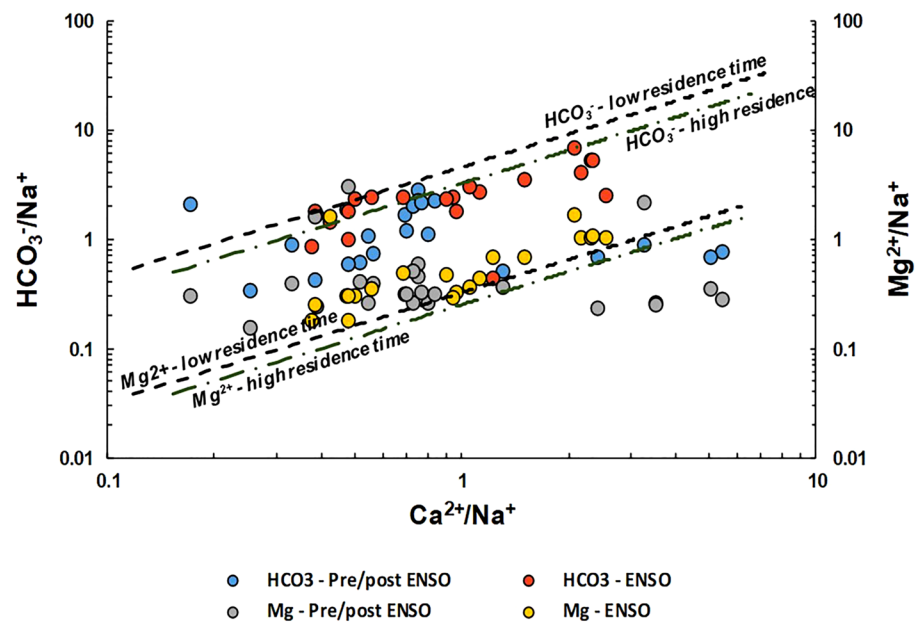
The scatter plot of Fig. 6 seeks to approach the provenance of dissolved phases in the middle Paraná River during the 1982–1983 flood. The record has been separated into one set including data preceding and following the flood (i.e., lower discharges) and another set collected during the high flood. Most of the plotted data is bounded within four straight lines resulting from the chemical reconstruction of source minerals in the Sierra Nevada (California and Nevada, USA) (Garrels and Mackenzie 1967). Two lines represent the ideal hydrolysis of a mixture of plagioclase (175 mol) + biotite (14 mol) + calcite (115 mol) + $\text{H}_2\text{O} + \text{CO}_2$ under conditions of deep circulation (i.e., groundwater, extended rock–water interaction). One line stands for the covariation of HCO_3^- and Ca^{2+} , whereas the other represents the covariation of Mg^{2+} and Ca^{2+} , both normalized to Na^+ .

The other two lines represents the ideal dissolution occurring in near surface conditions, of a combination of plagioclase (177 mol) + biotite (7.3 mol) + potassium feldspar (13 mol) + $\text{H}_2\text{O} + \text{CO}_2$ (i.e., ephemeral springs, limited water–rock interaction) (Garrels and Mackenzie 1967). As in the previous instance, one stands for the covariation of HCO_3^- and Ca^{2+} , whereas the other represents the covariation of Mg^{2+} and Ca^{2+} , both normalized to Na^+ .

The scattering of the data suggests a pronounced lithological variability in the sources, as well as dilution, and unevenness in the rock–water interaction. The dynamic exchange between the floodplain and the main channel is also a likely significant cause.

According to Gaillardet et al. (1999), waters draining limestone/carbonate would plot at or near the upper right corner of the graph, whereas waters draining hypersaline terrains/evaporites would fall in the graph's lower left corner. Solutes from pure silicates sources would plot above

Fig. 6 Mixing diagram using Na-normalized Paraná River water molar ratios. The lines show ideal trends for diverse weathering products and residence times. Data were separated into sets collected during the high flood, and preceding and following the event. Notice logarithmic axes. See text for explanation



the uppermost lines, with $\text{Ca}^{2+}/\text{Na}^+$ plotting in the $\sim 0.3\text{--}0.7$ range.

Revisiting the main hydro chemical characteristics during high flooding

Table 1 shows data gathered between 1981 and 1984, when the Paraná River was subjected to one of the highest (and most disastrous) floods on record: the ENSO-set off exceptional flood of 1982–1983 (e.g. Depetris and Kempe 1991). Table 1 presents variables and parameters herein chosen to project an image of the system’s response to extreme flooding.⁵

During the high flood, data showed that a five-fold increase in discharge (i.e., from 10000 to 50000 $\text{m}^3 \text{s}^{-1}$, at the Corrientes gauging station) determined a mean TDS dilution of $\sim 350\%$. Average conductivity (i.e., corrected for temperature) fell from ~ 225 to $64 \mu\text{S cm}^{-1}$. The coefficient of determination⁶ ($r^2 = 0.402$) for the nonlinear regression implies that only $\sim 40\%$ of the variability of the total dissolved solids (TDS) is accounted for by the discharge determined at the Corrientes stage meter and that other factors would explain the remaining $\sim 60\%$ of the variance of the dependent variable. Likewise, in Fig. 7a, ionic strength peaks ($7\text{--}8 \text{ mM}$) at low discharge and then sharply decreases ($1\text{--}2 \text{ mM}$) with high flooding, reaching values close to those exhibited by rainfall. Along this line of argumentation, the

Na^+/Cl^- molar ratio in Paraná River water (Fig. 7b) exhibited a mean of 0.76 ± 0.8^7 during several months previous to the high flood, and reached a mean of 1.4 ± 0.9 during the ENSO-triggered flood. The inundation left a lasting “memory effect”, because after the event, the Na^+/Cl^- molar ratio in river water (Fig. 7b) reached a mean of 1.3 ± 0.3 , which persisted for several months. It must be emphasized that, according to Möller (1990), the Na^+/Cl^- molar ratio of continental rainfall fluctuates between 1.1 and 1.8 (i.e., not influenced by excess Na and Cl), although the molar Na^+/Cl^- ratio in bulk maritime rainwater is ~ 0.86 .

Meybeck (2005) used the parameter TZ^+ [$\text{TZ}^+ (\text{meq L}^{-1}) = \text{Na}^+ + \text{K}^+ + 2\text{Ca}^{2+} + 2\text{Mg}^{2+}$] to interpret river chemistry. Some samples analyzed in the Paraná during the 1982–83 flood plot within the *dilute* field ($0.375 < \text{TZ}^+ < 0.750 \text{ meq L}^{-1}$), although most samples measured during the flood fall within the *medium dilute* field ($0.750 < \text{TZ}^+ < 1.500 \text{ meq L}^{-1}$), and only two samples plot in the *medium mineralized* domain ($1.500 < \text{TZ}^+ < 3.000 \text{ meq L}^{-1}$). The samples determined before and after the ENSO flood are more concentrated to some extent, reaching the *mineralized* field ($3.000 < \text{TZ}^+ < 6.000 \text{ meq L}^{-1}$) at low flow (Fig. 8). In this instance, flood-induced dilution obviously explains low concentrations. Some *medium mineralized* waters were probably accounted for by the relative increase in the water volume supplied by the Paraguay River system (i.e., the upper Paraguay plus its Andean tributaries). At any rate, Figs. 7 and 8 are examples of the low correlation that prevails between river discharges and physicochemical variables, which is

⁵ Additional chemical information collected during the SCOPE/UNEP Carbon Project is included as supplementary material.

⁶ The statistic r^2 is the proportion of the variance in the dependent variable that is predictable from the independent variable.

⁷ Mean \pm standard deviation.

Table 1 (continued)

Date	Discharge (Q) ^a (m ³ /s)	Stage height La Paz (cm)	Stage height Rosario (cm)	WSS (cm Km ⁻¹)	pH	Ionic strength (mM)	Alkalinity (meq L ⁻¹)	SO ₄ ²⁻ (mM)	Cl ⁻ (mM)	Ca ²⁺ (mM)	Mg ²⁺ (mM)	Na ⁺ (mM)	K ⁺ (mM)	TZ ⁺ (meq L ⁻¹)	DIC (mM)	DOC ^b (μM)	PCO ₂ ^b (ppmv)	TSS ^b (mg L ⁻¹)	POC/PN ^b	POC ^b (μM)	PN ^b (μM)
26.10.83	32273	2117	819	3.9	6.86	0.832	0.36	0.030	0.181	0.129	0.074	0.170	0.026	0.602	0.49	1632	3748	63	10.3	109.9	10.7
06.12.83	27378	2079	784	3.9	6.71	1.077	0.41	0.054	0.248	0.155	0.103	0.209	0.049	0.773	0.59	250	7444	106	8.8	151.5	17.1
15.12.83	26229	2069	775	3.9	6.62	1.257	0.31	0.163	0.209	0.190	0.082	0.270	0.036	0.849	0.48	375	15063	499	9.0	258.1	28.6
06.04.84	17880	1980	693	3.8	7.72	1.634	0.74	0.100	0.214	0.287	0.103	0.339	0.036	1.155	0.76	433	769	265	5.6	362.2	64.3
30.05.84	18616	1989	702	3.9	7.17	1.408	0.62	0.076	0.209	0.237	0.095	0.304	0.046	1.013	0.69	941	2079	201	5.1	159.9	31.4
01.08.84	13908	1921	640	3.7	7.26	1.234	0.68	0.004	0.237	0.060	0.098	0.344	0.038	0.698	0.17	325	1853	88	nd	nd	nd
25.09.84	15226	1942	659	3.8	7.82	1.063	0.56	0.020	0.209	0.147	0.091	0.309	0.026	0.810	0.58	275	455	81	nd	nd	nd
29.11.84	20060	2007	718	3.8	7.27	1.016	0.53	0.018	0.226	0.132	0.078	0.335	0.036	0.791	0.60	291	1782	116	nd	nd	nd

^aAt Corrientes (1200 km from mouth)

^aEl Niño lasted between April 1982 and July 1983

^bDepetris and Kempe 1993; nd: not determined

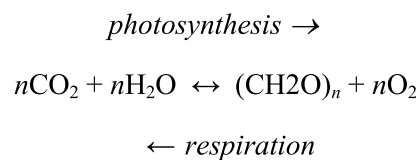
another characteristic feature—besides pronounced dilution—of high floods in large rivers with vast flood plains.

Particulate matter transported in suspension (TSS) also shows ample variability, as dissolved phases do. Relatively low TSS concentrations are ubiquitous during the flood, reaching values that were common before the flooding event (Fig. 9a). The highest concentrations are reached in the ~ 17000–30000 m³ s⁻¹ flow range, regardless the conditions governing the discharge (i.e., before, during the flood, or afterwards). These concentrations are probably caused by the flushing out of the floodplain.

Particulate organic carbon (POC) is also very variable in all river stages (Fig. 9b), although this characteristic is particularly noticeable in the ~ 17000–30000 m³ s⁻¹ discharge span, where organic matter sources may be terrestrial debris as well as phytoplankton. At high discharges (Q > 35000 m³ s⁻¹) POC concentration remains < ~ 100 μM and POC/PN maintains the mixed sources signatures for the transported organic matter (Fig. 9b).

Probing further into the high-flood discharge vs. concentration, it is important to explore the influence of WSS in governing the hydro chemical dynamics during exceptional flooding and the role played by the water exchange mechanism with the floodplain.

WSS appear to show a discernible linkage with some biogeochemical variables in as much the former is associated with the draining of the floodplain. Dissolved inorganic carbon [DIC = (CO₂ (aq)) + (H₂CO₃) + (HCO₃³⁻) + CO₃²⁻]⁸ is a relevant example. Figure 10 shows the clustering of DIC concentrations that prevailed preceding the flood (i.e., Pre-ENSO), whereas higher concentrations are recorded during the flood and after its occurrence, when the floodplain is drained due to higher WSS and decreasing water level. Increased heterotrophic respiration in the floodplain water bodies leads to increased DIC by supplying CO₂:



The well-known mechanism is further corroborated in Fig. 11. The level reached by the CO₂ partial pressure (PCO₂) in Paraná's flood water supplied another angle to understand the flooding/draining process of the floodplain. PCO₂ is very high during the high flood and after its occurrence, when the floodplain is drained as a consequence of increased WSS associated with decreasing water levels. Figure 11 also shows exceedingly high PCO₂ values

⁸ (CO₂ (aq)) + (H₂CO₃) are often expressed as (CO₂^{*}).

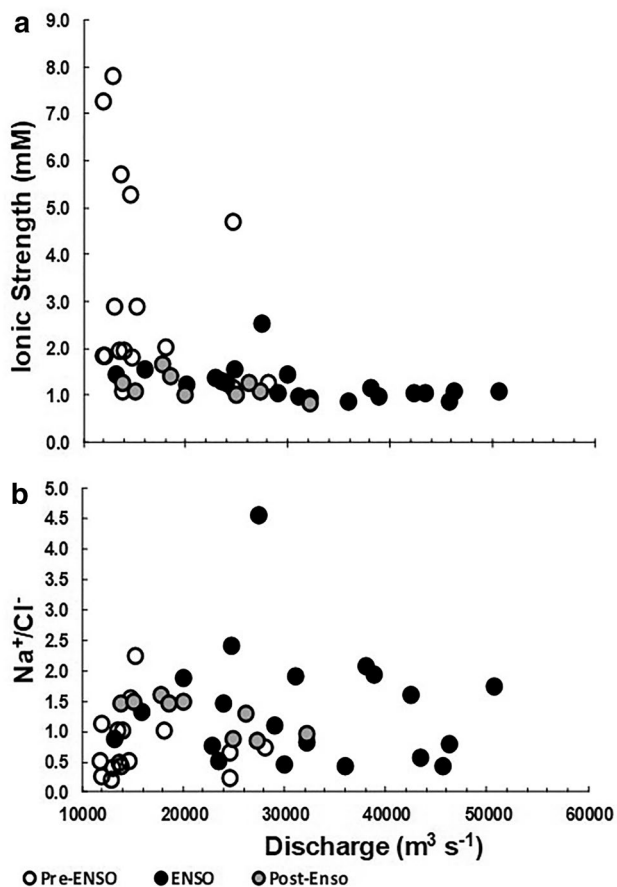


Fig. 7 Variability of ionic strength (a) and Na^+/Cl^- ratio (b) in the middle Paraná River. Points are divided into data collected preceding and following the high flood, and during the event. Mean discharge for the period was $\sim 17000 \text{ m}^3 \text{ s}^{-1}$

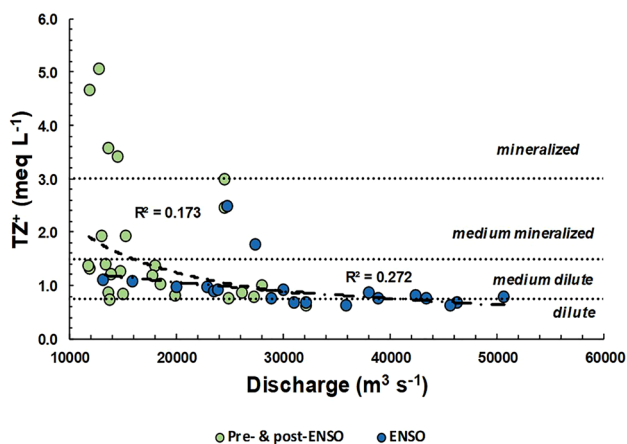


Fig. 8 TZ^+ variability during the ENSO-triggered flood, and data collected preceding and following the event. Notice the dilution effect during the high flood. Mean discharge for the period was $\sim 17000 \text{ m}^3 \text{ s}^{-1}$

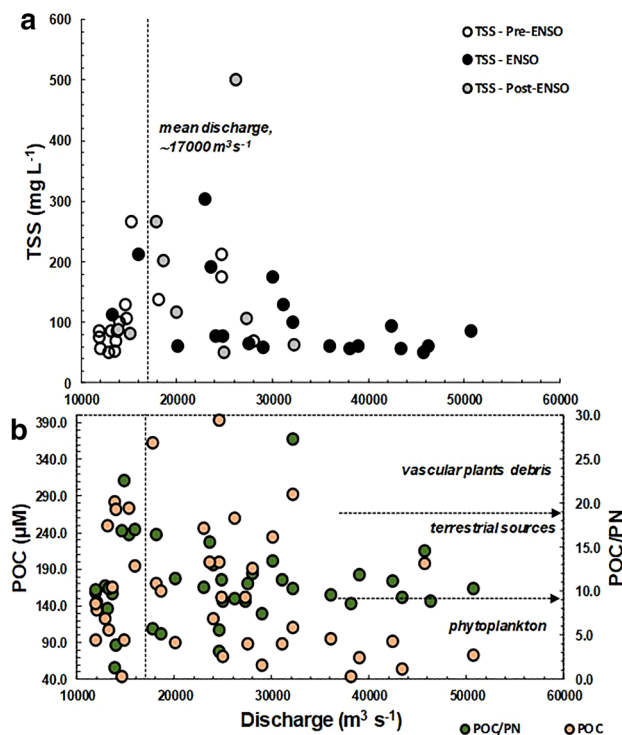
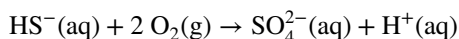


Fig. 9 a Total suspended solids (TSS) variability in the middle Paraná River. Notice dilution at high flow. **b** POC and POC/PN (in TSS) in the middle Paraná River. Note the dominance of phytoplankton and terrestrial sources during high discharges. Data from Depetris and Kempe (1993)

(~ 8000 – ~ 16000 ppmv)⁹ associated with above-the-mean discharges (i.e., $> 17000 \text{ m}^3 \text{ s}^{-1}$). The wide span of the variation leads to different scenarios: one when the river was in the rising limb (lower PCO_2), and another when discharge was in the downward limb of the hydrograph.

Accordingly, the dynamics of the flood determined a decrease in pH to below-neutral values when overbank discharge reached $\sim 20000 \text{ m}^3 \text{ s}^{-1}$ and flood water, mainly acidified by the high PCO_2 increase and other processes occurring in the wetland, was flushed out from the flood valley (Fig. 12). As water level decreased and organic-rich ox-bows and ponds in the riparian environment became shallower, the oxidation of sulfur may have also contributed to lower the pH:



The dynamics of carbon and its sources in the Paraná River has shown, among other findings that dissolved organic carbon (DOC) and the inorganic fraction (DIC) were essentially uncorrelated with Paraná’s discharge during the 1981–1984 period (i.e., 1982–1983 ENSO flood included) (Fig. 13): DOC showed high concentrations associated with

⁹ ppmv = parts per million in volume.

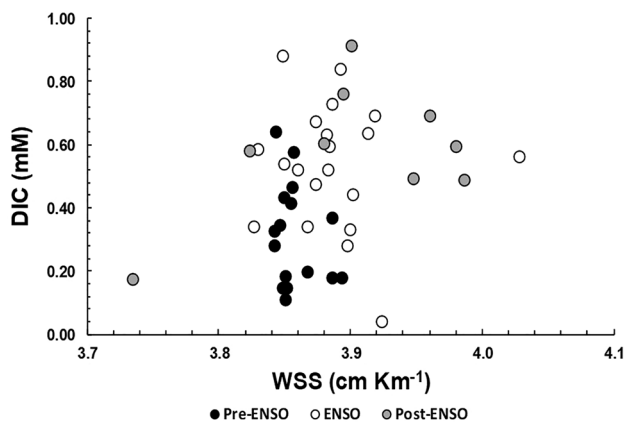


Fig. 10 Relationship between WSS and DIC. Notice clustering of data points preceding and following the ENSO event

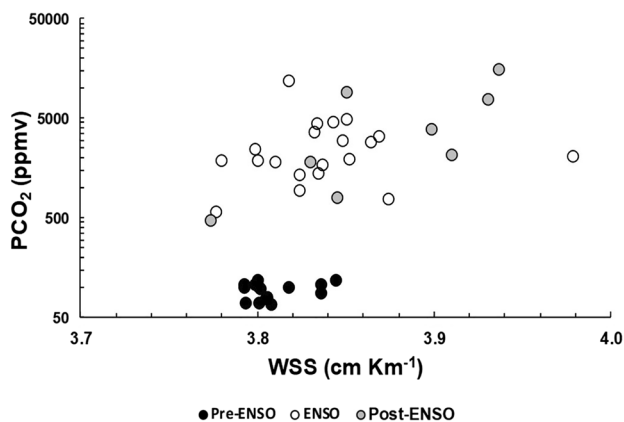


Fig. 11 Relationship between WSS and PCO₂ in the middle Paraná River. Observe clustering of data points preceding the high flood and the very high PCO₂ values following the event, when the floodplain was being drained. Note logarithmic y-axis

both, low and high discharges, whereas DIC exhibited a narrower variability. In fact, the coefficient of variation (i.e., $c_v = \sigma/\mu$) for DOC was ~ 0.87 , and $c_v \approx 0.47$ for DIC. Furthermore, the DIC/DOC ratio was 0.4 ± 0.34 for the period preceding the flood, 1.14 ± 0.7 during the high flood, and 1.68 ± 1.0 after the flood. These values further suggest that bacterial respiration is a significant part of DIC in the water drained from the riparian environment.

Table 2 shows contrasting dynamics for some important biogeochemical parameters during the pre-ENSO, ENSO, and post-ENSO (flood) periods. TDS, TZ⁺, and DOC showed dilution throughout the flooding process, whereas DIC and PCO₂ exhibited an increasing concentration trend during the whole 1982–1983 flooding event. Clearly, the

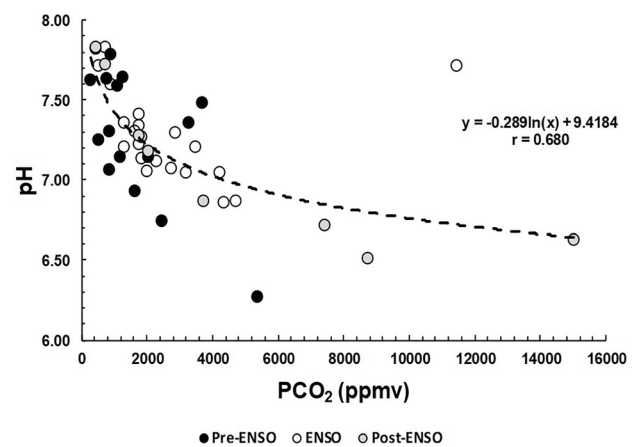


Fig. 12 Scatter diagram of PCO₂ and pH in the middle Paraná River. Very high partial pressures and pH < 7.0 are associated with the draining of the floodplain

contribution of PCO₂ to DIC appeared as more important during the flood and in the following receding stage than in the preceding period.

Scientific literature shows that the silica cycle has significant overlap with the carbon cycle (e.g., Berner et al. 1983). In the riverine environment, SiO₂ is particularly subjected to biological consumption (e.g., diatoms, radiolarians) and to other physicochemical reactions, particularly while river water remains isolated in the lentic environment. The dynamic water exchange between floodplain and the river main channel during the Paraná's flood of 1982–1983 revealed, however, a discernible signal. Preceding the high flood, the geometric mean of SiO₂ concentrations (\pm standard deviation of normalized data) was $229 \pm 1.3 \mu\text{mol L}^{-1}$; during the ENSO-caused flood, the concentration increased to $265 \pm 1.1 \mu\text{mol L}^{-1}$, and during the receding stage it decreased to $178 \pm 1.4 \mu\text{mol L}^{-1}$. Since apparently there was no significant dilution after the high flood, the decrease observed during the declining stage can only be attributed to the dilution exerted by SiO₂-depleted flood plain water entering the main stem.¹⁰

Within the framework of the SCOPE-UNEP Carbon Project, a downriver biogeochemical probe was performed in July–August 1985, after the high flood of 1982–1983 (Table 3). The attention was placed on the biogeochemistry of carbon (Depetris and Kempe 1993) even though other hydro chemical data was also collected. The downriver survey showed a generalized concentration increase—in the upper as well as in the middle Paraná River reaches—in most dissolved chemical elements, with some conspicuous exceptions (e.g., PO₄³⁻) (Depetris and Pasquini 2007;

¹⁰ The differences among geometric means were statistically significant.

Fig. 13 Variability of DOC and DIC against discharge in the middle Paraná River, during the 1982–83 ENSO-triggered high flood. Note highly variable DOC and more uniform DIC. DOC moderate-to-high concentrations (> 10 mg L⁻¹) are probably associated with riparian zone waters entering the main river stem

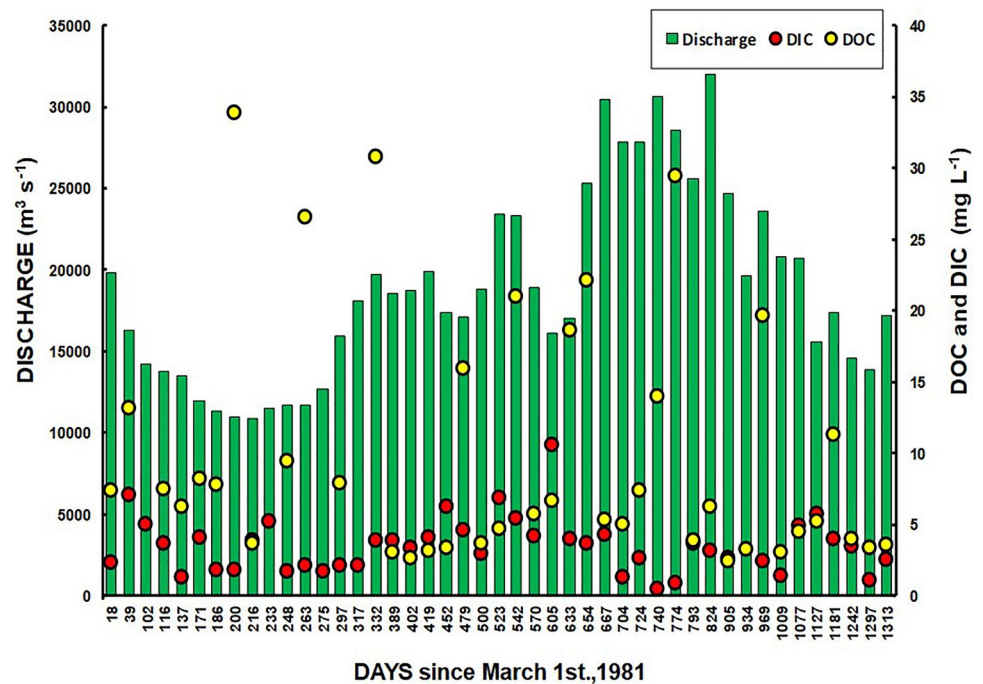


Table 2 Mean concentrations in the middle Paraná

	Pre-ENSO	ENSO	Post-ENSO
TDS (mg L ⁻¹)	116.1 ± 1.8	60.4 ± 1.3	57.9 ± 1.2
TZ ⁺ (µeq L ⁻¹)	1899.4 ± 1.7	867.6 ± 1.4	811.6 ± 1.2
DIC (µM)	267.4 ± 1.7	459.1 ± 1.2	538.2 ± 2.0
DOC (µM)	884.3 ± 2.0	556.5 ± 2.2	422.7 ± 1.9
PCO ₂ (ppmv)	1268.2 ± 2.2	2166.7 ± 1.4	2745.4 ± 3.2

River during the high flood (1982–1983 ENSO), and the preceding and following periods

Geometric means ± geometric SD

Pasquini and Depetris 2012). In general, these investigations showed the geochemical influence of the Paraguay River and its tributaries, not only in the dissolved and particulate inorganic load of the middle Paraná stretch but also in its carbon biogeochemistry (Depetris and Kempe 1993). More recent studies (Campodonico et al. 2015, 2016) also showed that physicochemical inhomogeneity is not only observed downriver but also crosswise. This transverse chemical asymmetry is mainly caused by the incomplete mixing of the Paraguay and Paraná rivers, which is perceived for over 200 km downstream their meeting point (Campodonico et al. 2015). The use of ²²²Rn also showed the likelihood of modest groundwater contributions (Campodonico et al. 2015).

Figure 14 illustrates the influence of the Paraguay River on the Paraná’s middle section by means of TZ⁺ parameter. It also shows the effect of the floodplain’s lotic and lentic environments on the river’s main stem. Table 3 shows

how inorganic constituents can be concentrated by evapotranspiration, and how biogeochemical components can be altered while isolated in the riparian environment. Similarly, Bonetto et al. (1998), and Villar et al. (1998) have compared the hydrochemistry of the lower Paraná’s main stem and the adjacent swampy floodplain and have shown the biogeochemical changes—particularly concerning nutrients—experimented in the riparian environment of the lowermost Paraná’s reach.

Long-term variability of solute concentration in the Paraná River

As has been described, the concentration of dissolved and particulate phases in the middle Paraná River water is, in general, poorly correlated with discharge, partly due to the water exchange process (i.e., regulated by stage height) between the main channel and the riparian zone. Flood water—while in the floodplain—endures chemical (e.g., it may concentrate and precipitate mineral phases), biological (e.g., biological production regulates dissolved gases), and physical (e.g., turbidity and color affect light penetration) changes while residing—for weeks or months—in the riparian environment. When the mass of water stored in the floodplain for a relatively long period of time re-enters the

Table 3 Paraná River downstream hydro chemical data

River/ environment	Date	Dist to mouth (Km)	Site	Temp. Water ^b (°C)	pH ^b	Eh _{oxi} (mV)	Eh _{red} (mV)	Cond _{total} ^c (µS cm ⁻¹)	Cond _{calc} (µS cm ⁻¹)	Ionic strength (mM)	TSS ^b (mg L ⁻¹)	O ₂ ^b per cent sat.	DOC ^b (µM)	DIC (µM)	Alkalinity (meq L ⁻¹)	Cl ⁻ (µM)	SO ₄ ²⁻ (µM)	Ca ²⁺ (µM)	Mg ²⁺ (µM)	Na ⁺ (µM)	K ⁺ (µM)	TZ ⁻ (µeq L ⁻¹)	CO ₂ (µM)
Paraná	22.07.85	1882	Pto. Esperanza	19.3	6.60	383	232	44.5	46.9	0.5658	1.8	128	142	210.6	0.13	175	43.7	65.4	66.2	93.1	37.9	392.5	78.6
Paraná	22.07.85	1822	Montecarlo	19.4	6.70	325	232	43.5	52.8	0.6577	1.64	110	183	13.3	0.01	170	116.2	77.6	65.4	92.6	38.6	406.5	4.3
Paraná	23.07.85	1583	Posadas	18.5	6.70	380	231	45.5	47.7	0.5762	1.1	113	108	253.9	0.17	175	31.9	70.1	66.6	99.2	37.9	409.1	82.2
Paraná	23.07.85	1244	P. de la Patria	19.5	6.90	364	230	54.0	49.6	0.6074	5.8	103	117	275.6	0.21	158	33.6	73.1	68.7	113.5	38.1	433.6	65.5
Paraná	24.07.85	1032	Beña Vista	19	6.50	308	232	61.5	62.6	0.7454	63.5	109	216	189.8	0.11	265	70.1	87.6	81.4	132.2	43.2	510.0	81.3
Paraná	25.07.85	957	Goya	18.2	6.50	340	231	84.0	157.1	1.825	63.7	118	n.d.	661.7	0.38	44	275.0	111.5	101.6	886.43	56	1352.6	282.8
Paraná	25.07.85	853	Esquina	18.3	6.80	300	231	69.0	69.0	0.7997	42.7	127	325	146.5	0.11	339	59.4	94.1	88.9	149.2	48.6	560.6	40.4
Paraná	30.07.85	600	Paraná	17.5	6.85	345	231	78.0	186.9	2.604	70.2	92	283	361.3	0.27	457	437.4	602.4	94.6	156.2	52.7	1536.2	90.3
Pond	24.07.85	1030	P. Cuá	19.5	6.60	295	232	135.0	186.5	2.263	0.93	145	n.d.	269.4	0.17	880	259.8	176.4	320.9	512.01	63.7	1538.3	98.5
Stream	24.07.85	1030	P. Cuá	18.5	6.30	310	231	143.0	201.1	2.353	38.7	83	458	697.7	0.32	948	226.4	155.9	300.3	735.1	74.7	1696.4	375.9
Pond	25.07.85	870	Aguará	17.5	6.70	298	231	65.0	75.3	0.8948	34.1	137	233	120.7	0.08	305	112.2	97.6	86	195.7	47.8	604.9	39.3
Iguazú	21.07.85	1930	Falls	19.2	7.10	428	232	35.0	37.6	0.5561	2.7	101	142	120.7	0.10	135	38.9	52.7	51.4	80	26.36	313.2	19.2
Paraná-Guazú	22.07.85	1800	Pte. ruta	20.5	7.00	327	233	46.0	49.3	0.5911	n.d.	115	142	219.8	0.18	203	22.0	76.3	69.9	99.2	33.8	424.2	41.4
Paraguay	23.07.85	1210	P. de la Patria	18.8	6.50	332	232	122.0	164.9	1.991	84.6	78	416	477.9	0.27	705	214.4	138.2	275.6	509.8	71.4	1385.8	202.7
Comenies	25.07.85	853	Pte. ruta	n.d.	6.10	335	231	70.0	76.7	0.8431	22.8	94	425	184.8	0.06	339	108.7	73.9	48.5	342.3	32.2	616.1	121.1

Note: light grey corresponds to flood plain's lentic/lotic environments; darker grey corresponds to tributaries
n.d.: not determined. ^b Depetris and Kempe 1993

Light grey corresponds to flood plain's lentic/lotic environments; darker grey corresponds to tributaries

^aDepetris and Kempe (1993)

main channel, it modifies the river water physicochemical signature.

The availability of a 10-year long, uninterrupted time series (Lenardón 1979), allowed to further explore aspects of the discharge-concentration relationship. A relevant example is depicted in Fig. 15, where mean Cl⁻ and TDS concentrations are plotted against river discharge. Over the 10-year period, TDS exhibited a weak correlation with discharge ($r=0.16$, $p<0.1$) and, hence, a very low percentage of its variance is accounted for by the independent variable. On the other hand, the correlation of Cl⁻ (i.e., considered a conservative element) with discharge is higher than with TDS ($r=0.45$, $p<0.001$) and the independent variable (i.e., discharge) accounts for ~20% of its variability. The relationship is not linear and deviates markedly—as all large rivers do—from the ideal dilution model (i.e., twice the discharge leads to one-half the solute concentration). During the 1982–1983 flood, most of the Cl⁻ concentration variance remains unaccounted for, inasmuch river discharge “explains” only ~24% of its variability.

Figure 16 shows the monthly variation of discharge and alkalinity during the 10-year period (1965–1975) used to analyze the discharge–alkalinity relationship in the middle Paraná. A cursory inspection of the graph appears to show that the coherence between discharge and alkalinity is somewhat restricted to high water events (e.g., the strong El Niño-triggered floods of 1966 and 1973). Other floods (or low-water periods), not necessarily connected with ENSO events, may or may not be correlated with alkalinity concentration. Although reduced during low river stages, the connections between the floodplain and the main stem remain almost permanently operative. High alkalinity concentrations are also discernible associated with some low-discharge periods (e.g., often connected with La Niña events). During such phases, the relative importance of the Bermejo and Pilcomayo rivers as discharge

suppliers to the middle Paraná increases, as also does carbonate alkalinity.

Moreover, correlation between both, alkalinity and discharge, is not significant ($p>0.01$). Correlations were low between discharge and other variables routinely used in water analysis, like, TDS—as seen above—turbidity ($r=-0.148$, $p<0.05$), and filtered water color ($r=0.471$, $p<0.001$) (Lenardón 1979).

Alkalinity and the factors affecting its concentration in the middle Paraná River

Properly defined, total alkalinity is “the equivalent sum of the bases that are titratable with a strong acid” (e.g., Stumm and Morgan 1996, Albarède 2009). In terms of molar concentrations, total alkalinity (A_T) is equal to,

$$A_T = m(\text{HCO}_3^-) + 2m(\text{CO}_3^{2-}) + m(\text{B}(\text{OH})_4^-) + m[\text{H}_3(\text{SiO})_4^-] \\ + m(\text{HS}^-) + m(\text{organic anions}) + m(\text{OH}^-) - m(\text{H}^+),$$

where m is the molar concentration. In most natural waters, only carbonate and bicarbonate ions are of significance, because, in comparison, the other ions exhibit very low concentrations. Accordingly, the previous equation shortens to:

$$A_T \approx m(\text{HCO}_3^-) + 2m(\text{CO}_3^{2-})$$

Therefore, in most natural waters, total alkalinity is approximately equal to carbonate alkalinity (e.g., Drever 1997; Langmuir 1997). However, in large rivers with extensive floodplains (e.g., the Paraná River), where large water volumes may be stored for significant periods of time, a number of processes, which may modify alkalinity concentration may grow in importance and contribute to the modification of alkalinity concentration.

Given the lithology and climate dominating Paraná's western upper catchments (i.e., the Bermejo and Pilcomayo rivers),

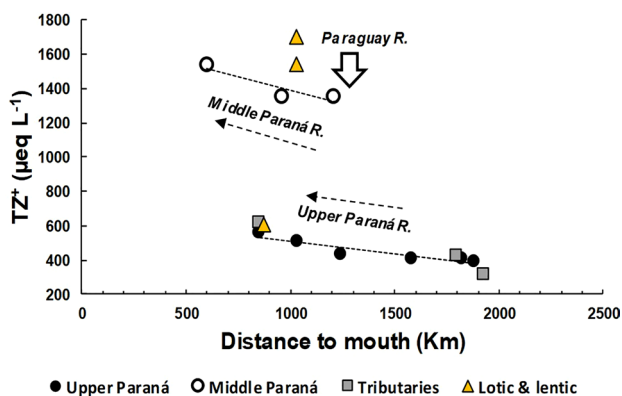
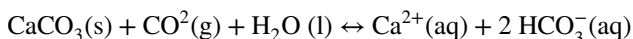
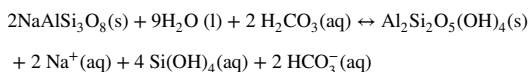


Fig. 14 Variation of TZ^+ as a function of the downriver distance to the mouth. Notice the discontinuity imposed by the Paraguay River. The Paraguay River chemical signal is preserved in the western margin, whereas the Upper Paraná’s persists in the eastern one

it is likely that the prevailing reaction controlling A_T production in the Andean headwaters might be the dissolution of carbonate rocks, which results in increased A_T :



Likewise, in the Brazilian and Paraguayan tropical headwaters, rock weathering (i.e., hydrolysis of silicates) is surely important, in reactions like the weathering of plagioclase, which also increases A_T :



Upon completion, this well-known reaction produces kaolinite as the only solid product. Other reactions, such as nitrification and denitrification—among others—may contribute to increase or decrease A_T in the Paraná’s main stem.

The 10-year long data time series (Lenardón 1979) was employed to approach the interpretation of the discharge–alkalinity relationship in the middle Paraná River. To improve its understanding, the following graph (Fig. 17) was constructed with A_T geometric means and discharge (Q) values for an average year. (i.e., of the studied period, 1965–1975).

A significant covariance between Q and A_T is observable in Fig. 17 for the period January–July. Summer (austral) rains mobilize the products of mineral weathering in the drainage basin which are, most likely, the main factors increasing A_T . It is probable that during the first half of the year, average A_T is basically carbonate alkalinity, which distinctively covariates with mean monthly Q. At peak discharge, it is noticeable a lag between both variables: mean Q leads mean A_T , reaching its maximum in March, whereas A_T attains its peak concentration in April. This lag between discharge and concentration of different chemical species in

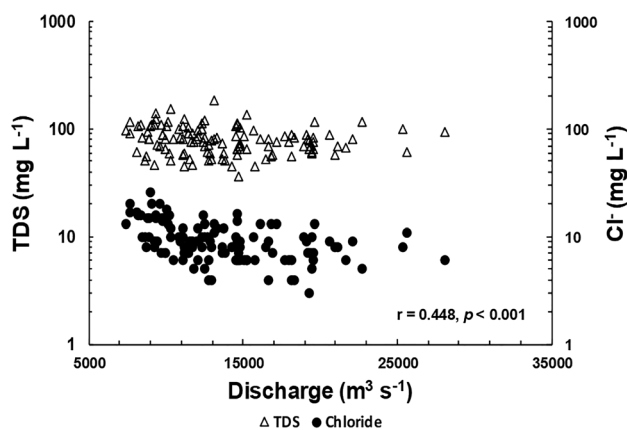
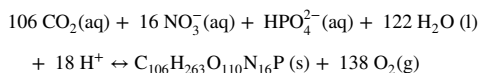


Fig. 15 Variability of TDS and Cl^- concentration as a function of discharge. Data are a 10-year long time series (1965–1975) gathered in the middle Paraná River (600 km upstream the mouth). Cl^- shows a low correlation with discharge. In the nonlinear relationship, discharge accounts for ~24% of Cl^- variability. Mean discharge for the 1965–75 decade was ~14500 $m^3 s^{-1}$. Note logarithmic axes

river water has been observed and studied for several decades (e.g., Godsey et al. 2009; Hunsaker and Johnson 2017).

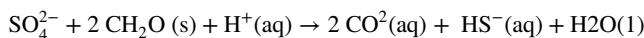
During (austral) winter and early spring, both variables diverge markedly. As considered before, low water stage in the middle Paraná means that the abundant lotic and lentic water bodies in the Paraná’s floodplain undergo a draining process—activated by increasing WSS—and a very substantial water volume is reintroduced into the main channel (i.e., likely over 10% of the river discharge).

During the time spent in the floodplain’s riparian scenario, the stored water experienced several biogeochemical modifications and, therefore, the flashed out floodplain water bears a different signature, particularly through several reactions that affect alkalinity. For example, due to the consumption of H^+ , A_T increases through denitrification and by means of the assimilation of nitrate ions into photosynthesis:



Supporting this view, Villar et al. (1998) found, in lentic bodies of the lower reach of the Paraná River (i.e., downstream Rosario, 420 km upstream the mouth), a fast decrease in NO_3^- concentrations in lentic waters, suggesting large losses by denitrification. Likewise, Bonetto et al. (1998) found a $N-NO_3^-$ concentration of $20 \pm 8 \mu g L^{-1}$ in marshy environments, and $197 \pm 18 \mu g L^{-1}$ in the main river channel.

Another mechanism likely to participate in A_T increase is the reduction of SO_4^{2-} , which may participate in relatively deep (i.e., anoxic) water bodies:



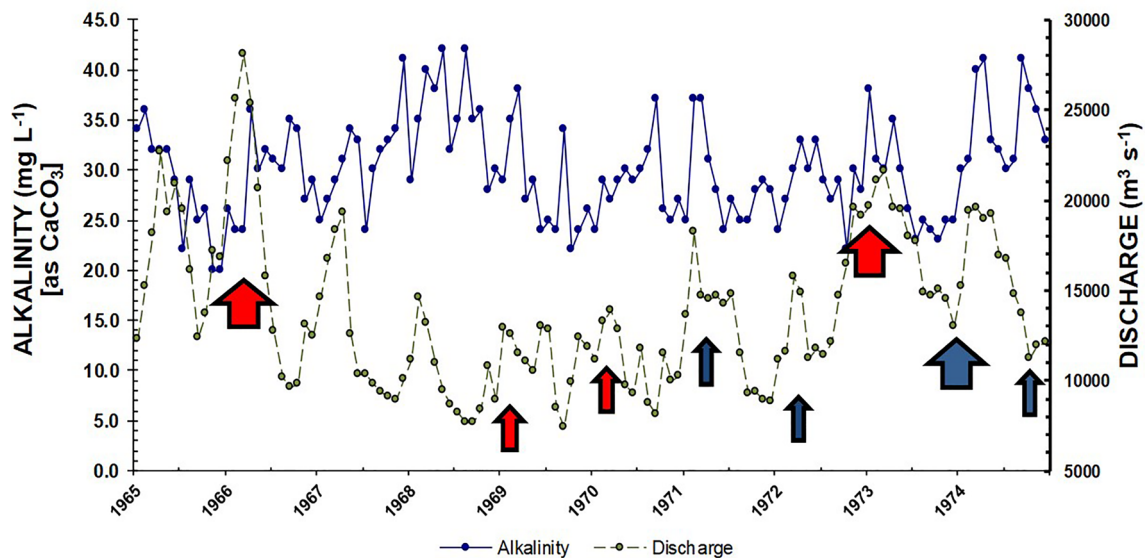


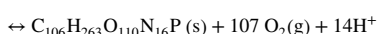
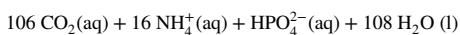
Fig. 16 Variability of alkalinity and discharge in the middle Paraná River (600 km upstream the mouth). Red arrows correspond to EL Niño events and blue arrows to La Niña. The thickness of the arrows

is proportional to the magnitude of each event. Mean discharge for the 1965–1975 decade was $\sim 14500 \text{ m}^3 \text{ s}^{-1}$

Bonetto et al. (1998), in the comparison of lentic and lotic environments in the Paraná's lower reach, found a significant decrease in SO_4^{2-} concentration ($5.4 \pm 0.8 \text{ mg L}^{-1}$) in floodplain's marshy environments as compared with the concentration recorded in the main river channel ($8.4 \pm 1.0 \text{ mg L}^{-1}$). The CO_2 concentration increase observed in Fig. 11 further endorses the likelihood of the occurrence of reduction reactions. It may partially explain the high PCO_2 levels reached during the post-flood draining of the riparian zone.

In September, austral spring restarts the assimilation of NO_3^- associated with the photosynthesis processes, causing A_T to increase due to H^+ consumption; A_T -rich waters due to the stimulated photosynthetic activity in riparian ponds and ox-bows (i.e., turbidity decreases in stagnant waters and primary productivity increases), re-enters the Paraná's main stem. Additionally, reduced discharge frequently accompanies increased concentrations of the nutrient pool. Villar et al. (1998) have shown that—in the Paraná's lower reach—concentrations of soluble reactive phosphorous were higher in the floodplain's lotic bodies than in the main channel.

Nonetheless, the processes of photosynthesis and respiration are coupled by assimilation of NO_3^- , NH_4^+ , and HPO_4^{2-} . The assimilation of NH_4^+ during photosynthesis causes the production of protons, which directs to a decrease of A_T in the floodplain's ponds and oxbows and, hence, in the water masses, introduced later into the main stem:



In November–December, Q started a swelling rate and A_T also began the austral summer incipient increasing trend, mobilizing the products of rock weathering (i.e., due to summer rains) and dissolution of carbonate rocks in the river's upper catchments.

The mean hydrograph obtained for the 1965–1975 time period, and the average A_T computed for each month of the synthetic hydrological year, allowed to produce the scatter graph of Fig. 18. The graph shows that, in general, A_T tends to decrease with below-the-mean Q ,¹¹ whereas the trend becomes positive for above-the-mean discharges. It has been shown above that low discharges stimulate the draining of the floodplain's lotic and lentic water bodies, where different biogeochemical processes define changes in the chemical composition of the temporarily stored water mass, which is reintroduced in the main channel during the decreasing stage. This is the reason why the mean A_T concentrations of August, September, and October are clustered in the decreasing trend of Fig. 18. It seems plausible to assume that in the middle Paraná River, during the low-water months, floodplain-supplied A_T masks to a certain extent the A_T signal brought downstream from upper reaches.

¹¹ The mean discharge in the middle Paraná River for 1965–1975 was $\sim 14500 \text{ m}^3 \text{ s}^{-1}$. Discharges began to increase in the 1970s and, currently, mean annual discharge reaches $\sim 17000 \text{ m}^3 \text{ s}^{-1}$ (e.g., Pasquini and Depetris 2007).

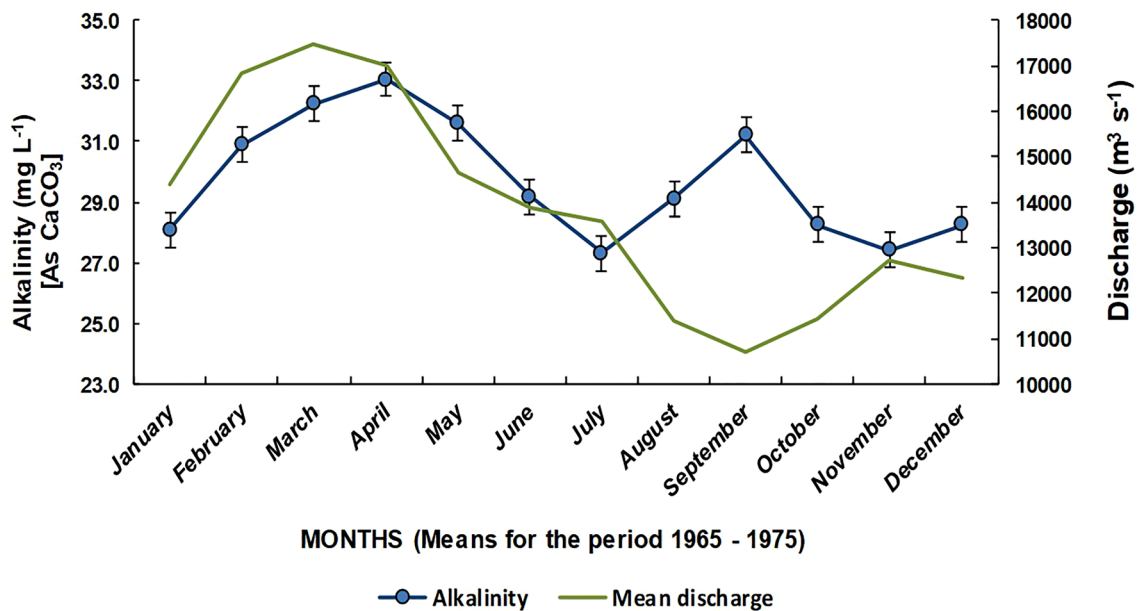


Fig. 17 Variability of mean monthly discharge and mean monthly alkalinity in the middle Paraná River (600 km upstream the mouth) during the 1965–1975 decade [basic data from Lenardón (1979)]. Mean river discharge for the analyzed 10-year period was ~14500

m^3s^{-1} . Error bars (computed for alkalinity) are the standard error of the mean [i.e., (also called standard deviation of the mean), $s_{\bar{x}} = s/n^{1/2}$, where s is the sample standard deviation and n is the number of observations]

Summarizing and concluding remarks

The Paraná River is among the largest fluvial systems in the Americas with tropical as well as Andean semiarid headwaters. Most of its present course originated in the Late Cretaceous, in irregular synchrony with the opening of the Atlantic Ocean (Potter and Hamblin 2006). Its hydrology exhibits a working teleconnection with the occurrence of ENSO phenomena in the Pacific, which usually results, with average frequency of two to seven years, in high floods (El Niño) or atypical low discharges (La Niña) (e.g., Depetris et al. 1996). High floods affect, above all, the middle and lower Paraná, which is characterized by a vast floodplain. Yearly inundations impact in various ways on the riparian environment that blankets the flood valley, particularly from a biogeochemical point of view. Hydrological seasonality rules a dynamic water exchange between lentic environments prevailing in the flood valley, and lotic conditions of countless streams that carve the floodplain, and the main river stem.

The upper Paraná River supplies 65–75% of the middle stretch discharge, whereas the Paraguay—and mainly its Andean tributary, the Bermejo River—deliver a similar proportion of the total solid load. Therefore, the middle Paraná water has a chemical signal which is similar to the upper Paraná, while the geochemical signature of the sediment load conveys a dominant Andean mark. This characteristic is shown by using $^{87}\text{Sr}/^{86}\text{Sr}$ and $^{143}\text{Nd}/^{144}\text{Nd}$, which

separates the provenance of water and sediment into different sources. A Na-normalized mixing diagram shows that most water samples plot within the boundaries determined by the ideal dissolution lines of mixed minerals, suggesting as well, the occurrence of a varied residence time pattern in the rock-water interaction.

Data gathered during the 1982–1983 ENSO-triggered flood showed that among its main effects was TDS dilution, decreasing concentrations from ~225 to ~64 $\mu\text{S cm}^{-1}$ during the peaking flood. Most conspicuous was the marked decrease in pH (~6.5), concurrent with an extraordinary increase of PCO_2 (~16000 ppmv), caused by flood water which had been stored in lentic water bodies for significant periods of time and flowed back into the main stream following the high stage. The Paraná River, like any river (e.g., Butman and Raymond 2011), but particularly those with vast flood valleys with abundant riparian vegetation, tends to be CO_2 -supersaturated when compared with the atmosphere. The Parana is, therefore, a permanent source of atmospheric CO_2 but—as shown—its evasion was especially significant during the 1982–1983 extraordinary flood.

Water mostly remained in the *medium dilute* water-type (Meybeck 2005) throughout the inundation period,

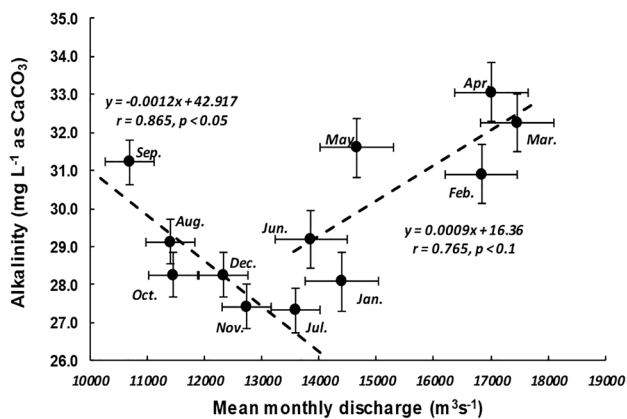


Fig. 18 Scatter graph relating mean monthly discharges (i.e., the synthetic hydrograph for 1965–1975) and the corresponding monthly mean alkalinity concentrations. The breaking point is close to the mean discharge computed for the period (i.e., $\sim 14500 \text{ m}^3\text{s}^{-1}$). Error bars are the standard error of the mean

dominated by alkalinity among the negatively charged components. The correlation of discharge and solutes concentration became blurred during the high flood, and Cl^- concentrations, which frequently exhibits significant coherence with discharge, is a good example of the above assertion. The interpretation of this image is that, in the middle Paraná River and during high floods -and after their occurrence-, concentrations are controlled by the dynamic water exchange between the main channel and the contiguous wetland.

In low-slope rivers with fully developed floodplains—like the Paraná—WSS is an important factor during flooding, because its fluctuations usually accompany the inundation and drainage of the floodplain during high flood events. The control of WSS is particularly evident with DIC and PCO_2 , when high concentrations are reached at peaking flood, and during the descending stage, when flood water is drained from the vast wetland.

DOC shows high concentration during both, low and high water. These episodes of high concentrations (~ 20 – 35 ppm, or ~ 1.7 – 2.9 mM) alternate with somewhat extended periods of relatively constant low concentrations. These peak concentrations are interpreted as sporadic DOC contributions from the wetland. On the other hand, DIC remained relatively constant throughout the flood and the preceding low-water stage, leading to conclude that DOC was not mainly respired and converted into CO_2 by bacteria. Therefore, the already mentioned high PCO_2 originates, most likely, in the respiration of primary heterotrophs mainly consuming particulate organic debris (Depetris and Kempe 1993).

A long series (1965–1975) of continuous discharge and solute measurements performed in the middle Paraná River (Lenardón 1979) was used to develop a scheme to elucidate the role played by water level variability during floods and

the concentration of alkalinity, which is a chemical variable that—in wetlands—plays an important role in the biogeochemistry of carbon.

Several biogeochemical reactions occurring mostly in the Paraná's lentic realm—fully developed in the riparian zone—appear to be significant factors in controlling the variability of A_T concentrations determined in the middle Paraná main stem or riparian lotic system. Photosynthesis/respiration, nitrification/denitrification, and sulfide oxidation/sulfate reduction are mechanisms that, superimposed on the main processes supplying A_T in a fluvial system (i.e., rock weathering reactions) can increase or decrease A_T depending on the hydrological stage. Although the relative significance of each mechanism remains unknown, this exercise should be seen as an approach to understand the association between the river's fluctuating hydrological stage and the resulting biogeochemical processes.

References

- Albarède F (2009) *Geochemistry. An Introduction*, 2nd ed. Cambridge University Press, Cambridge
- Baca P (2008) Hysteresis effect in suspended sediment concentration in the Rybárik basin, Slovakia. *Hydrol Sci J* 53(1):224–235
- Benke AC, Chaubey I, Ward MG, Dunn EL (2000) Flood pulse dynamics of an unregulated river floodplain in the southeastern U.S. coastal plain. *Ecology* 81(10):2730–2741
- Berner R, Lasaga A, Garrels R (1983) The carbonate-silicate geochemical cycle and its effect on atmospheric carbon dioxide over the past 100 million years. *Am J Sci* 283(7):641–683
- Bonetto C, Villar C, de Cabo L, Vaithyanathan P (1998) Hydrochemistry of a large floodplain river. *Verh Int Verein Limnol* 26:899–902
- Butman D, Raymond PA (2011) Significant efflux of carbon dioxide from streams and rivers in the United States. *Nat Geosci*. <https://doi.org/10.1038/NGEO1294>
- Campodonico VA, García MG, Pasquini AI (2015) The dissolved chemical and isotopic signature down flow the confluence of two large rivers: the case of the Paraná and Paraguay rivers. *J Hydrol* 528:161–176
- Campodonico VA, García MG, Pasquini AI (2016) The geochemical signature of suspended sediments in the Paraná River basin: implications for provenance, weathering and sedimentary recycling. *CATENA* 143:201–214
- Ceballos DS, Frangi J, Jobbágy EG (2013) Soil volume and carbon storage shifts in drained and afforested wetlands of the Paraná River Delta. *Biogeochem* 112:359–372
- Davis JC (1986) *Statistics and data analysis in geology*, 2nd edn. Wiley, Chichester
- De Cabo L, Seoane R (2005) Suspended sediments in the Bermejo River and their impact on the hydrochemistry of the lower Paraná River. *IAHS-AISH Publ* 294:151–158
- Degens ET, Kempe S, Richey JE (1991) *Biogeochemistry of major world rivers*. SCOPE 42. Wiley, Chichester
- Depetris PJ (1976) *Hydrochemistry of the Paraná River*. *Limn Oceanogr* 21(5):736–739
- Depetris PJ (2005) Revisiting biogeochemical aspects of the Paraná River. In: Heathwaite L, Webb B, Rosenberry D, Weaver D, Hayashi M (eds) *Dynamics and biogeochemistry of river corridors*

- and wetlands. International Association of Hydrological Sciences, Wallingford, pp 159–166
- Depetris PJ, Kempe S (1991) The impact of the El Niño 1982 event on the Paraná River, its discharge and carbon transport. *Palaeogeogr Palaeoclimatol Palaeoecol* 89:239–244
- Depetris PJ, Kempe S (1993) Carbon dynamics and sources in the Paraná River. *Limnol Oceanogr* 38:382–395
- Depetris PJ, Paolini JE (1991) Biogeochemical aspects of South American Rivers: The Paraná and the Orinoco. In: Degens ET, Kempe S, Richey JE (eds) *Biogeochemistry of major world rivers*. SCOPE 42. Wiley, Chichester
- Depetris PJ, Pasquini AI (2007) The geochemistry of the Paraná River: an overview. In: Iriondo MH, Paggi JC, Parma MJ (eds) *The Middle Paraná River: limnology of a subtropical wetland*. Springer, Heidelberg, pp 143–174
- Depetris PJ, Kempe S, Latif M, Mook WG (1996) ENSO-controlled flooding in the Paraná River (1904–1991). *Naturwissen* 83:127–129
- Drever JI (1997) *The geochemistry of natural waters. Surface and groundwater environments*, 3rd edn. Prentice-Hall, Upper Saddle River
- Dunne T, Aalto RE (2013) Large river floodplains. In: Shroder J, Wohl E (eds) *Treatise on geomorphology*, vol 9. Academic Press, San Diego, pp 645–678
- Faure G (1986) *Principles of isotope geology*, 2nd edn. Wiley, New York
- Gaillardet J, Dupré B, Louvat P, Allègre CJ (1999) Global silicate weathering and CO₂ consumption rates deduced from the chemistry of large rivers. *Chem Geol* 159:3–30
- Garrels RM, Mackenzie FT (1967) Origin of the chemical composition of some springs and lakes. In: Gould RF (ed), *Equilibrium concepts in natural water systems*. Advances in Chemistry Series 67. American Chemical Society, Washington DC, pp 222–242
- Gili S, Gaiero DM, Goldstein SL, Chemale F, Jweda J, Kaplan MR, Becchio RA, Koester E (2017) Glacial/interglacial changes of Southern Hemisphere wind circulation from the geochemistry of South American dust. *Earth Planet Sci Lett*. <https://doi.org/10.1016/j.epsl.2017.04.007>
- Godsey SE, Kirchner JW, Clow DW (2009) Concentration-discharge relationships reflect chemostatic characteristics of US catchments. *Hydrol Process* 23:1844–1863
- Hansen DV (1990) Physical aspects of the El Niño event of 1982–1983. In: Glynn PW (ed) *Global ecological consequences of 1982–83 El Niño–Southern Oscillation*. Elsevier, Amsterdam, pp 1–20
- Henry F, Probst JL, Thouron D, Depetris PJ, Garçon V (1996) Nd–Sr isotopic compositions of dissolved and particulate material transported by the Paraná and Uruguay rivers during high (December 1993) and low (September 1994) water periods. *Sci Géol Bull* 49:89–100
- Hunsaker CT, Johnson DW (2017) Concentration-discharge relationships in headwater streams of the Sierra Nevada, California. *Water Resour Res* 53:7869–7884
- Iriondo MH, Paggi JC, Parma MJ (eds) (2007) *The Middle Paraná River: limnology of a subtropical wetland*. Springer, Berlin
- Langmuir D (1997) *Aqueous environmental geochemistry*. Prentice-Hall, Upper Saddle River
- Lenardón AML 1979. Computer analysis of sequential hydro-chemical data. Its application for the Paraná River. Dissertation, Facultad de Ingeniería Química, Universidad Nacional del Litoral, Santa Fe, Argentina (in Spanish)
- Meybeck M (2005) Global occurrence of major elements in rivers. In: Drever JI (ed) *Surface and Ground Water, Weathering, and Soils*, vol 5. Elsevier, Amsterdam, pp 207–223
- Michaelis W, Ittekkot V (1982) Biochemistry of rivers: field and analytical techniques. In: Degens ET (ed) *Transport of carbon and minerals in major world rivers. Part 1*. Mitt Geol-Paläont Inst Univ Hamburg. SCOPE/UNEP Sonderb, pp 59–68
- Milliman JD, Farnsworth KL (2011) *River discharge to the coastal ocean*. Cambridge UP, Cambridge
- Möller D (1990) The Na/Cl ratio in rainwater and the seaside chloride cycle. *Tellus* 42B:254–262
- Muste M, Lee K (2013) Quantification of hysteretic behavior in stream-flow rating curves. Proc 2013 IAHR World Congress, <https://doi.org/10.13140/2.1.1302.3369>
- Paira AR, Drago EC (2007) Origin, evolution and types of flood plain water bodies. In: Iriondo MH, Paggi JC, Parma MJ (eds) *The middle Paraná River: limnology of a subtropical wetland*. Springer, Berlin, pp 53–81
- Pasquini AI, Depetris PJ (2007) Discharge trends and flow dynamics of South American rivers draining the southern Atlantic seaboard: an overview. *J Hydrol* 333:385–399
- Pasquini AI, Depetris PJ (2010) ENSO-triggered exceptional flooding in the Paraná River: where is the excess water coming from? *J Hydrol* 383:186–193
- Pasquini AI, Depetris PJ (2012) Hydrochemical considerations and heavy metal variability in the middle Paraná River. *Environ Earth Sci* 65:525–534
- Potter PE, Hamblin WK (2006) *Big rivers worldwide*. Brigham Young University, Geology studies, Provo
- Potter PE, Maynard JB, Depetris PJ (2005) *Mud & mudstones. Introduction and overview*. Springer, Berlin
- Richards K, Brasington J, Hughes F (2003) Geomorphic dynamics of floodplains: ecological implications and a potential modelling strategy. *Freshwat Biol* 47(4):559–579
- Rollinson H (1993) *Using geochemical data: evaluation, presentation, interpretation*. Longman, Harlow
- Sanci R, Panarello HO (2018) Distribution and isotopic signature of deep gases in submerged soils in an island of the Lower Delta of the Paraná River, Argentina. *Environ Monit Assess* 190(11):647
- Sarachick ES, Cane MA (2010) *The El Niño–Southern Oscillation phenomena*. Cambridge UP, Cambridge
- Soldano FA (1947) Régimen y aprovechamiento de la red fluvial argentina. Parte I. El río Paraná y sus tributarios. Ed. Cimera, Buenos Aires (In Spanish)
- Steiger J, Tabacchi E, Dufour S, Corenblit D, Peiry J-L (2005) Hydrogeomorphic processes affecting riparian habitat within alluvial channel-floodplain river systems: a review for the temperate zone. *River Res Appl* 21:719–737
- Stone RC, Hammer GL, Marcussen T (1996) Prediction of global rainfall probabilities using phases of the Southern Oscillation Index. *Nature* 384:252–255
- Stumm W, Morgan JJ (1996) *Aquatic chemistry. Chemical equilibria and rates in natural waters*. Wiley, New York
- Tank JL, Rosi-Marshall E, Griffiths NA, Entekin SA, Stephen ML (2010) A review of allochthonous organic matter dynamics and metabolism in streams. *J N Am Benthol Soc* 29(1):118–146
- Villar CA, de Cabo L, Vaithyanathan P, Bonetto C (1998) River-floodplain interactions: nutrient concentrations in the Lower Paraná River. *Arch Hydrobiol* 142:433–450
- Walling DE, Webb BW (1988) The reliability of rating curve estimates of suspended sediment yield: some further comments. In: Bordas M P, Walling D E (eds) *Sediment budgets*. IAHS 174, Wallingford, pp 337–350

Publisher's Note Springer Nature remains neutral with regard to jurisdictional claims in published maps and institutional affiliations.